Hydraulics Research
Wallingford

CURRENT-DEPTH REFRACTION OF WATER WAVES

A Description and Verification of Three Numerical Models

H N Southgate MA

Report No SR 14
January 1985

Registered Office: Hydraulics Research Limited,
Wallingford, Oxfordshire OX10 8BA.
Telephone: 0491 35381. Telex: 848552

ABSTRACT

This report describes three computational models for determining wave refraction by a combination of depth variations and currents. The theoretical formulation of current-depth refraction and the numerical procedures used in the models are described. The models are tested for some simple cases involving parallel depth contours and unidirectional currents for which analytical solutions are available.

The report was produced for the Water Directorate of the Department of the Environment under DOE Contract No. PECD 7/7/129.

CONTENTS

1 INTRODUCTION

The effects of waves and currents are important in many engineering applications. For example, knowledge of wave-current forces is needed to analyse the response of offshore structures, ships (berthed and under way), breakwaters, and coastal and harbour works. Knowing the wave current shear stress at the seabed is also essential to determining the concentration and movement of seabed material.

Often engineers have reasonably accurate knowledge of waves and currents separately, and can analyse their separate effects. However, in many applications it is advisable to consider the interaction between them. Significantly different results are usually obtained when the interaction between waves and currents is taken into account compared with simply adding their separate effects. This is true both of the forces exerted by waves and currents, and of the propagation of wave energy from one location to another when currents are present.

In this report we consider how wave-current interaction affects the propagation of waves in nearshore regions. The aim is to extend existing computational models of shallow water effects on waves (refraction, shoaling, bottom friction, breaking) to include the influence of currents. A complete description of wave-current interaction is not sought, and in any case would be mathematically intractable. Some simplifications are therefore assumed at the outset:

1. The effects of waves on currents are ignored. Such effects include rip currents from a beach, and the circulation induced by differences in set-up of the water level between areas of different wave height. Generally the effects of waves on currents are smaller than those of currents on waves and often, as in the case of rip currents, they are localised, small-scale effects.

2. Linear wave theory and the refraction approximation are assumed. This simplification is used in HR's existing ray tracing and finite difference models of wave propagation in coastal areas. The reason for this simplification is that it

allows currents to be introduced without the equations becoming too complex for a ready computational solution in general coastal situations. The refraction approximation does place some limits on the types of waves and bathymetry that can be modelled with reasonable accuracy. Generally the refraction approximation does not hold shorewards of the breaker zone, and will work best where variations in water depth are gradual and regular.

3. The currents are assumed to be vertically uniform and not varying with time.

4. The tests described in this report do not include dissipative phenomena. However, the theoretical formulation used allows terms to be introduced describing the energy losses due to bottom friction and wave breaking.

Existing wave models require gridded values of water depth over the studied sea area. The wave-current models will require, in addition, current magnitudes and directions to be specified in gridded form. In principle, currents from any physical source could be included, provided they are known in advance. However, many sources of currents such as wind-generated currents, wave-induced currents, currents arising from density variations etc, are difficult to determine over wide areas. Tidal currents, on the other hand, because of their periodicity, are usually predictable over large areas even where little tidal recording has taken place. In many nearshore regions of the world, and particularly around the British Isles, tidal currents are considerably more important than currents from other sources. It is envisaged therefore that tidal currents will be the main type of current used in these models.

The models are not site specific and are designed to be used in general coastal areas. There are no restrictions on the grid size per wavelength, other than giving an adequate representation of the bathymetry and current field. They can therefore be used with waves of any period and sea areas of any size.

2 THEORY

2.1 Introduction

The theory of wave-current interaction within the refraction approximation has been extensively reported in the recent technical literature (see for example references 1, 2, 3). A number of approaches have been tried; the approach using the concept of wave rays is perhaps the most general, and is the one most readily incorporated into existing pure-wave computer models. A number of further developments are needed for the purpose of adapting the theory to existing wave models in use at HR.

Wave-current interaction has been introduced into three of HR's pure-wave computer models, namely the foward-tracking ray model, the back-tracking ray model, and the finite difference model. Each of these pure-wave models caters for different coastal wave prediction problems, and descriptions of them can be found in references 4-9.

This section contains a summary of the derivation of the wave-current equations. Section 3 describes specific further developments needed to adapt this theory for the three types of computational model.

2.2 Definitions

In the following, the term "absolute" refers to quantities measured relative to the seabed, and "relative" to quantitites measured relative to an observer travelling with the local current. Definitions of symbols appear in the Appendix.

Figure 1 shows the definition of a wave ray. In contrast to pure waves, rays are not directed along orthogonals to wave fronts. Instead they are in the direction of travel of the absolute group velocity (equal to the vector sum of the current and the relative group velocity). The wave kinematics (i.e. determination of the ray paths) are treated first. The time-dependent governing equations are established and then particularised to the time-independent case, which is used in the models. The wave dynamics (i.e determination of wave energy) are then considered.

2.3 Wave Kinematics

We start from four basic equations which are derived from pure-wave refraction theory and simple kinematic considerations.

$$\underline{\nabla} \times \underline{k} = 0 \qquad \text{Eiconal Equation} \qquad (1)$$

$$\frac{\partial \underline{k}}{\partial t} + \underline{\nabla}\, \omega_a = 0 \qquad \text{Conservation of Wave Crest Equation} \qquad (2)$$

$$\omega_a = \omega_r + \underline{k} \cdot \underline{U} \qquad \text{Doppler Equation} \qquad (3)$$

$$\omega_r^2 = g\, k \tanh (kh) \qquad \text{Dispersion Equation} \qquad (4)$$

In these equations, ω_a is the absolute wave angular frequency, ω_r is the relative wave angular frequency, k is the wavenumber, h is the water depth, g is the acceleration due to gravity, U is the current velocity, and ∇ is the two-dimensional horizontal gradient operator. Underlined symbols represent vector quantities.

By eliminating ω_r between Eq 3 and Eq 4, the magnitude of the wavenumber k can be determined from the resulting equation by a Newton-Raphson iteration technique.

Substituting Eq 3 into Eq 2 and using Eq 1,

$$\left[\frac{\partial}{\partial t} + (\underline{c}_{gr} + \underline{U}) \cdot \underline{\nabla}\right] \underline{k} = \frac{\partial \omega_r}{\partial h}\, \underline{\nabla} h - (\underline{\nabla}\, \underline{U}) \cdot \underline{k} \qquad (5)$$

c_{gr} is the relative group velocity.

We can write Eq 5 as two equations involving the magnitude (k) and direction (α) of the wavenumber. This is done by taking scalar products with unit vectors in the orthogonal direction (s) and wave crest direction (f) respectively. The results are

$$\left[\frac{\partial}{\partial t} + (\underline{c}_{gr} + \underline{U}) \cdot \underline{\nabla}\right] k = -\frac{d\omega_r}{dh}\frac{dh}{ds} - \left[k_x \frac{\partial U_x}{\partial s} + k_y \frac{\partial U_y}{\partial s}\right] \qquad (6)$$

$$\left[\frac{\partial}{\partial t} + (\underline{c}_{gr} + \underline{U}) \cdot \underline{\nabla}\right] \alpha = -\frac{1}{k}\frac{\partial \omega_r}{\partial h}\frac{dh}{df} - \frac{1}{k}\left[k_x \frac{\partial U_x}{\partial f} + k_y \frac{\partial U_y}{\partial f}\right] \qquad (7)$$

The time-independent equations are obtained by putting $\partial/\partial t = 0$ and $\underline{c_{gr}} + \underline{U} = \underline{c_{ga}}$ in the above equation

$$\frac{dk}{dr} = -\frac{1}{c_{ga}} \frac{\partial \omega_r}{\partial h} \frac{dh}{ds} - \frac{1}{c_{ga}} \left[k_x \frac{\partial U_x}{\partial s} + k_y \frac{\partial U_y}{\partial s} \right] \tag{8}$$

$$\frac{d\alpha}{dr} = -\frac{1}{c_{ga} k} \frac{\partial \omega_r}{\partial h} \frac{dh}{df} - \frac{1}{c_{ga} k} \left[k_x \frac{\partial U_x}{\partial f} + k_y \frac{\partial U_y}{\partial f} \right] \tag{9}$$

In these equations, differentials of the depth (h) and the current quantities (U_x, U_y) are determined from the local depth and current values. $\partial \omega_r / \partial h$ is obtained by differentiation of the dispersion relation. The result is

$$\frac{\partial \omega_r}{\partial h} = \frac{g\, k^2 \left(1 - \tanh^2 (kh)\right)}{2 \omega_r} \tag{10}$$

The relative and absolute group velocities are given by

$$c_{gr} = \frac{\omega_r}{2k} \left(1 + \frac{2kh}{\sinh (2kh)}\right) \tag{11}$$

$$c_{ga}^2 = U^2 + c_{gr}^2 + 2U\, c_{gr} \cos (\delta - \alpha) \tag{12}$$

in which δ is the current direction.

We now have equations for determining the spatial rate of change of wavenumber (k) and orthogonal angle (α) in the ray direction (along r). However, since the solution process relies on tracing rays (not orthogonals), we need an expression for the rate of change of ray direction (μ) along r. We can derive this by using the relation between ray angle, and the current and orthogonal angles (see Fig 1).

$$\tan \mu = \frac{U \sin \delta + c_{gr} \sin \alpha}{U \cos \delta + c_{gr} \cos \alpha} \tag{13}$$

Differentiation of Eq 13 with respect to the ray direction (r) involves some algebra. The result simplifies to:

$$\frac{d\mu}{dr} = \frac{1}{c_{ga}^2}\left[U^2\frac{d\delta}{dr} + c_{gr}^2\frac{d\alpha}{dr} + Uc_{gr}\cos(\delta-\alpha)\left(\frac{d\alpha}{dr}+\frac{d\delta}{dr}\right)\right.$$

$$\left. + \sin(\delta-\alpha)\left(-U\frac{dc_{gr}}{dr} + c_{gr}\frac{dU}{dr}\right)\right] \qquad (14)$$

In this equation, differentials of U and δ are determined from local current values. $d\alpha/dr$ is given by Eq 9. The evaluation of dc_{gr}/dr requires further consideration. From Equations 4 and 11 we can write

$$c_{gr} = \frac{\sqrt{g\ k\ \tanh(kh)}}{2k}\left(1 + \frac{2kh}{\sinh(2kh)}\right) \qquad (15)$$

c_{gr} is a function of k and h only, and therefore

$$\frac{dc_{gr}}{dr} = \frac{\partial c_{gr}}{\partial k}\frac{dk}{dr} + \frac{\partial c_{gr}}{\partial h}\frac{dh}{dr} \qquad (16)$$

dk/dr is given by Eq 8, dh/dr is determined from local depth values, and $\partial c_{gr}/dk$ and $\partial c_{gr}/dh$ are found from differentiation of Eq 15. After some algebra the results are:

$$\frac{\partial c_{gr}}{\partial k} = \frac{c_{gr}}{2kT}\left[kh(1-T^2) - T\right] + \frac{\omega_r h\ (1-T^2)}{2kT}\left[T - kh(1+T^2)\right] \qquad (17)$$

$$\frac{\partial c_{gr}}{\partial h} = \frac{gk(1-T^2)}{2\omega_r}\left[\frac{T - kh(1+T^2)}{T} + \frac{k\ c_{gr}}{\omega_r}\right] \qquad (18)$$

where T = tanh (kh)

This completes the system of equations needed for determining the ray paths.

2.4 Wave Dynamics

The wave height is determined by the condition of conservation of wave action along rays

$$\frac{A^2\ c_{gr}\ b}{\omega_r} = \text{Constant} \qquad (19)$$

where b is the ray separation. References 10 and 11 contain derivations of this equation. The conservation of wave action can be expressed in other ways. Which of these is used depends on the numerical method adopted, and this will be considered in the next section.

3 NUMERICAL SOLUTION OF THE WAVE-CURRENT EQUATIONS

In this section we describe the adaptations to the theory needed for each of the three wave models.

3.1 Forward-Tracking Ray Model

The sea area under study is discretised with a set of grids, each composed of square elements. Field quantities (ie depths, current magnitudes and current directions) are input to the model as an array of values at the vertices in the grids. For the purpose of plotting rays across the grids, each square element is subdivided into two right-angled triangles. Field quantities and their spatial derivatives are determined at any point in a triangle by linear interpolation between the field values at the three vertices.

The technique of tracing rays across successive triangular elements is very similar to the pure-wave model (ref 7). However, there are some differences in the determination of the curvature of the ray paths. In the pure-wave model the interpolated quantity in each triangle is the wave celerity. With this assumption the ray curvature can be shown to be constant throughout the whole triangle (ref 8). Thus the ray paths are simply circular arcs and can be determined exactly. In the wave-current model, however, this is not the case, and the curvature of a ray path will change from point to point along the path within a triangle.

This difficulty can be overcome with an iteration process. When a ray enters a triangle, its curvature is calculated and assumed to be constant in the triangle. The exit point is determined and the curvature at that point calculated. Knowing the curvatures at the entry and exit point, an estimate can be made of the error in the ray path. If this error exceeds a certain level, the ray path is re-traced using the average of the curvatures at the entry and exit

points. This should give sufficient accuracy in most cases, but if necessary the process can be repeated further. In section 5.2 results are presented showing the effect of including the iterative step.

Eq 19 is used to determine wave heights along a ray. The constant is set at the start of each ray, and subsequent values of wave height along each ray are calculated from the local values of c_{gr}, ω_r and b. The first two of these quantities have already been determined in the ray tracing process (Eqs 12 and 4) but the ray separation b requires further calculation. For each ray, the ray separation can be determined, without reference to neighbouring rays, by solving numerically a second order ordinary differential equation along the ray (ref 3). However, a better method is to use a ray averaging process in each grid square (ref 12). If this is done, the ray separation does not have to be explicitly calculated. Further advantages of the ray averaging process are that ray crossings and caustics are automatically smoothed, and results are generated in a regular array over the whole studied sea area.

3.2 Back-Tracking Ray Model

The same considerations about representing field quantities, ray tracing, and iteration of ray curvature apply to the back-tracking model. However, a different method of calculating wave heights is used.

In the pure wave back-tracking model a fan of rays is traced from a single inshore point out to deep water in the opposite sense to the actual direction of travel of the waves (hence the name 'back-tracking' or 'reverse-tracking'. See Fig 3). In this method a wave spectrum in period and direction is considered, rather than the single periods and directions in the foward-tracking model. An offshore wave spectrum is specified, and the corresponding inshore spectrum is calculated using the condition of conservation of spectral density along each ray. This condition is slightly different to that for pure waves.

The conservation of spectral density in the wave-current case can be stated as

$$\frac{d}{dr}\left[\frac{S(k_x, k_y)}{\omega_r}\right] = 0 \qquad (20)$$

where k_x and k_y are the components of wavenumber in the co-ordinate directions. This condition follows from Liouville's Theorem in classical mechanics.

Since offshore spectra are usually given in terms of period (or frequency) and orthogonal angle, we require the spectral density in Eq 20 to be a function of these quantitites. We can obtain the relation between the two by equating infinitesimal elements.

$$S(k_x, k_y)\, dk_x\, dk_y = S(\omega_a, \alpha)\, d\omega_a d\alpha \qquad (21)$$

Now $dk_x\, dk_y = k\, dk\, d\alpha$

and, by differentiation of the Doppler equation Eq 3,

$$d\omega_a = (c_{gr} + U\cos(\delta-\alpha))\, dk$$

$$\text{Therefore } S(k_x, k_y) = \frac{c_{gr} + U\cos(\delta-\alpha)}{k} S(\omega_a, \alpha)$$

Substituting into Eq 20,

$$\left(\frac{c_{gr} + U\cos(\delta-\alpha)}{k\ \omega_r}\right) S(\omega_a, \alpha) = \text{Constant along a ray} \qquad (22)$$

The determination of the inshore spectrum and related statistical quantitites is identical to the pure-wave back-tracking model. It is important to remember that since rays are being traced backwards, the input current directions should be altered by 180^0 from their 'real life' directions.

3.3 Finite Difference Model

In the Finite Difference model, the governing refraction equations are solved by a finite difference scheme with nodes at the grid vertices. The offshore wave conditions (either a single period and direction or a spectrum) are specified at points along the row at the seaward edge

of the grid. A marching method is then used to calculate wave heights, periods and directions along successive rows. At each row an iterative process involving a predictor and corrector step is carried out. Details of the numerical scheme are the same as for the pure-wave model (ref 9) extended to include the additional variables in the wave-current case. The governing kinematic equations are the same as for the wave-current ray models, but the dynamic equations have a different form. This is considered below:

A differential form of Eq 19 is used for determining wave heights.

$$\underline{\nabla}. \left(\frac{A^2 \underline{c_{ga}}}{\omega_r}\right) = 0 \tag{23}$$

If dissipative effects are to be considered, a negative term is introduced on the right-hand side. Eq 23 can be expanded to give the rate of change of wave energy perpendicular to the rows (the x direction is along rows, and the y direction across rows).

$$\frac{\partial A^2}{\partial y} = \frac{1}{\sin \mu} \left[- \cos \mu \frac{\partial A^2}{\partial x} - A^2 \left(\cos \mu \frac{\partial \mu}{\partial y} - \sin \mu \frac{\partial \mu}{\partial x} + \frac{1}{c_{ga}} \frac{dc_{ga}}{dr} - \frac{1}{\omega_r} \frac{d\omega_r}{dr}\right)\right] \tag{24}$$

x derivatives are known from neighbouring values along rows. This leaves $\partial\mu/\partial y$, dc_{ga}/dr and $d\omega_r/dr$ to be determined. $\partial\mu/\partial y$ is found from knowing $d\mu/dr$ (Eq 14) and $\partial\mu/\partial x$

$$\frac{\partial \mu}{\partial y} = \frac{1}{\sin \mu} \left(\frac{d\mu}{dr} - \cos \mu \frac{\partial \mu}{\partial x}\right) \tag{25}$$

dc_{ga}/dr and $d\omega_r/dr$ are found from differentiation of Eqs 12 and 3 respectively. The results are:

$$\frac{dc_{ga}}{dr} = \frac{1}{c_{ga}} \left[(U + c_{gr} \cos(\delta - \alpha)) \frac{du}{dr} + (c_{gr} + U \cos(\delta - \alpha)) \frac{dc_{gr}}{dr} - U c_{gr} \sin(\delta - \alpha) \left(\frac{d\delta}{dr} - \frac{d\alpha}{dr}\right)\right] \tag{26}$$

$$\frac{d\omega_r}{dr} = -\cos(\delta-\alpha)\left(U\frac{dk}{dr} + k\frac{du}{dr}\right) + kU\sin(\delta-\alpha)\left(\frac{d\delta}{dr} - \frac{d\alpha}{dr}\right) \qquad (27)$$

4 TESTS WITH THE WAVE-CURRENT MODELS

4.1 Introduction

The verification of a mathematical model generally involves two stages. The first stage is to investigate how well the model predicts the exact solution of its governing equations. The second stage is to assess how good an approximation the governing equations are to a complete description of the physical processes occuring in nature. The tests described in this section are concerned with the first of these stages. The second stage, however, is usually more difficult. Generally speaking, since the wave-current models are based on a ray approximation, they will suffer much the same limitations as ray methods in the pure-wave case, plus some further restrictions relating to the modelling of the current field. An outline of some of these limitations has been given in the introduction to this report (Section 1). Much fuller discussions can be found in the technical literature (see for example references 2, 11 and 13).

4.2 Depth and Current Profiles

The three wave-current models have been tested with a simple bed bathymetry and current field. These tests, as well as demonstrating the accuracy of the models in their predictions of wave height and direction, are designed to show the sort of effects that currents can have on wave propagation.

The depth profile and grid used in these tests consist of a parallel contoured seabed covered by a grid of 24 by 9 square elements. The depth contours are parallel to the longer axis of the grid (x direction) and the depth values vary linearly from 15m to 5m along the shorter axis (y direction). Figure 2 shows the grid and depth contours. Despite its simplicity, a parallel contoured seabed is a good approximation to the depth profile in many coastal areas.

The current magnitudes vary linearly in the y direction from a value of $3ms^{-1}$ at the offshore boundary (the 15m depth contour) to $0.75ms^{-1}$

at the inshore boundary (the 5m depth contour). There is no variation of current magnitude in the x direction. The current directions are everywhere in the negative x direction (to the left in Figure 2).

The magnitudes of these currents are larger than commonly encountered in tidal regimes. These large currents have been chosen so that the performance of the models can be assessed in areas of strong current refraction which are unlikely to be exceeded in practice.

4.3 Tests Without Currents

A series of tests were carried out initially to check that the three types of model give correct pure-wave results when there is no current field. In the absence of currents, the wave height and direction at any point in the grid can be predicted from Snell's Law of refraction for given incident wave conditions. Each test was run at a period of 16s for a variety of incident wave angles (defined as the angle between the x axis and the forward ray direction, measured anticlockwise from the x axis). These tests are described below.

4.3.1 Back-Tracking Ray Model

A single run was performed, sending a fan of rays from one inshore point situated in the centre of the ninth row of squares. Rays were collected along the offshore boundary in angular 'boxes' of width 10°. These boxes were centred on values of 35°, 45°, 55° etc up to 145°. These central values therefore represent an average incident wave direction for each box. For each of these incident wave directions, wave heights and directions at the inshore point were determined.

It was expected that refraction effects would strongly reduce the number of rays in an offshore box compared to the number of rays setting out from the inshore point within the same angular range. The initial increment in angle between rays in the fan was therefore chosen as 0.125 degrees, a value which ensured a sufficient number of rays reached each offshore box.

4.3.2 Forward-Tracking Ray Model and Finite Difference Model

Six runs of each model were carried out for incident wave directions of 35°, 45°, 55°, 65°, 75° and 85° to correspond to results obtained in the back-tracking model. From the symmetry of the problem, incident angles between 95° and 145° would give the same results. In both models, results were obtained at points in a rectangular array covering the whole grid. However, these tests are essentially one dimensional (in the horizontal plane) and therefore identical results are expected from point to point along each row. An important difference between the models is that the ray model gives results at the centres of the square elements while the finite difference model gives results at the grid intersections. Inshore results from the finite difference model are therefore an average of values in rows either side of the square elements for which ray model results are quoted. Inshore results are obtained in the middle of the ninth row of squares, corresponding to the back-tracking tests.

4.4 Tests With Currents

The current field (defined in Section 4.2) was now used in the models, and the same series of tests as in the no-current case was carried out. The inclusion of currents meant that there were some differences in the tests.

When currents are included it is necessary to make the distinction between wave orthogonals and wave rays when specifying wave directions (in the pure-wave case orthogonals and rays are coincident). In all three models, the incident wave directions are specified as orthogonal directions. These are converted to ray directions in the models, and the rays are then traced across the grid. In the finite difference model, ray paths are not explicitly determined but rates of change of various quantities along ray directions are calculated. On output, ray directions are converted back to orthogonal directions.

The presence of the current field means that the problem is no longer symmetric for incident orthogonal directions either side of 90°. Twelve runs, instead of six, were therefore carried out with the forward-tracking ray model and finite difference model, for incident wave directions between 35° and 145° inclusive at 10° intervals. For

this current field, however, the problem remains one dimensional and identical results can be expected at all points on each row. Snell's Law can be extended to include the effects of this current field, thereby giving an analytical solution for this problem.

Fig 3 shows the ray paths from the back-tracking model using this current field. Fig 4 shows three sets of ray paths using the forward-tracking model.

5 DISCUSSION OF RESULTS

5.1 Agreement Between Models and Analytical Solution

Table 1 shows inshore wave heights for the pure-wave tests. Agreement between the models and the analytical solution is very good, with the forward-tracking and back-tracking ray models agreeing to within 0.5% of the analytical value for all incident wave directions. The finite difference model gives results somewhat lower than the analytical solution, the worst difference being about 2%.

The same trends in wave height error are apparent when the current field is introduced (Table 3). The forward-tracking and back-tracking ray models are slightly less accurate in comparison with the pure-wave tests. The forward-tracking wave heights are all within 1% of the analytical solution, while the back-tracking values differ by up to 2%. The finite difference model displays similar accuracy to the pure-wave tests.

Table 2 shows inshore wave orthogonal directions for the pure-wave tests. There is excellent agreement between all the models and the analytical solution for all incident directions. With currents present (Table 4), all the models show a similar very good agreement with the analytical solution.

From these results it can be concluded that the effects of quite strong current refraction, combined with depth refraction, are accurately represented in all three models.

5.2 Inclusion of Iterations

In earlier sections it was shown that an iterative procedure could be included in all three models to improve their accuracy. In Section 3.1, we showed that an iterative procedure could be used to improve the prediction of the ray paths in the forward-tracking and back-tracking ray models. In Section 3.3, we saw that the corrector step in the predictor-corrector method could be repeated to give greater accuracy. Tables 3 and 4 show the effects of including these iterative procedures.

Table 3 indicates that including the iteration step in the forward-tracking ray model has very little effect on the predicted wave height (less than 0.2%). With the back-tracking model, the effect is slightly greater for some incident wave directions (up to 1%). It can be seen that in some cases the iteration step actually makes the wave heights agree less well with the analytical values. However, this might be expected since the very small adjustments in wave height are likely to be outweighed by the errors in the ray counting processes which are present in the two ray models. These ray counting processes can produce errors of up to 1% for the ray densities used in the tests, and these errors are essentially random. The inclusion of the second corrector step in the finite difference model makes no difference to the wave height results.

The influence of the iteration step on predicted orthogonal directions is shown in Table 4. In contrast to the wave heights, the iteration step shows a consistent, though small, improvement for the two ray models. In both models the difference is as much as half a degree, and in most cases the iteration step brings the orthogonal directions closer to the analytical values. In the finite difference model there is no effect on orthogonal direction.

In conclusion, we see that the iteration step has a negligible effect on the prediction of wave heights in the forward-tracking and back-tracking ray models, but gives a small improvement to the predicted orthogonal directions. The inclusion of a second corrector step in the finite difference model has no effect on either wave height or orthogonal direction.

5.3 Effects of Currents on Wave Refraction

The influence of currents on the wave orthogonal directions is shown by comparing Tables 2 and 4. From these tables it can be seen that the effect of the current field is to reduce refraction for incident orthogonal directions less than 90° and to increase refraction for directions greater than 90°. This behaviour can be predicted by the following reasoning.

For incident orthogonal directions less than 90°:

(a) Considering current effects only. As the wave propagates across the grid, the wavenumber tends to decreases. This is by virtue of (1) the current opposing the wave direction and (2) the current strength decreasing. A decrease in wavenumber in turn means (from Eq 1) that the orthogonal direction decreases.

(b) Considering depth effects only. There will be depth refraction causing the orthogonal direction to increase.

(c) Considering current effects on depth refraction. With the current field present we would expect larger wavenumbers everywhere compared with the pure-wave case. These larger wavenumbers mean that depth refraction will be weaker than the pure-wave case, and therefore orthogonal directions will increase less rapidly.

Effects (a) and (c) act together and show that we would expect a net decrease in orthogonal angle (ie reduced refraction) in the currents case compared with the pure-wave case.

For incident orthogonal directions greater than 90°:

(a) Considering current effects only. As the wave propagates across the grid, the wavenumber tends to increase. This is because (1) there is a component of the current in the same direction as the waves and (2) the current strength decreases. An increase in wavenumber in turn means that the orthogonal angle increases.

(b) Considering depth effects only. There will be depth refraction causing the orthogonal direction to decrease.

(c) Considering current effects on depth refraction. With the current field present we would expect smaller wavenumbers everywhere compared with the pure-wave case. These smaller wavenumbers mean that depth refraction will be stronger than the pure-wave case, and therefore orthogonal directions will decrease more rapidly.

Effects (a) and (c) now act against each other. It is not clear therefore whether we would expect a net increase or decrease in orthogonal angle in the currents case compared with the pure-wave case. However, whichever occurs, we would expect the change to be smaller than it was for incident orthogonal directions less than 90°, where effects (a) and (c) acted with each other. In fact we see from Tables 2 and 4 a net decrease in orthogonal angle (ie stronger refraction). We also note, as predicted, that the change is smaller than for the case with incident orthogonal directions less than 90°

It can be seen that an attempt to predict the behaviour of orthogonal directions requires careful reasoning even in this simple example. Predictions of changes in wave height are more difficult still. One has to consider the effects of refraction, shoaling and Doppler shift, which are all affected by ray and orthogonal directions, the local current field, and depth variations. This multiplicity of factors can give rise to some surprising and apparently paradoxical results. A good illustration of an apparent paradox is shown in Fig 4. This figure shows three sets of ray paths in the forward-tracking model.

Top picture: Ray paths for incident orthogonal direction of 45° with current field to left.

Middle Picture: Ray paths for incident orthogonal direction of 45° with no currents.

Bottom Picture: Ray paths for incident orthogonal direction of 45° with current field to right.

The bottom picture is equivalent to an incident direction of 135° with currents to the left, but is presented as the mirror image for ease of comparison with the other two pictures. Note that in the top picture the initial ray direction is greater than 45° while in the bottom picture the initial ray direction is less than 45°.

Let us ask which of the three pictures we would expect to give the largest wave heights at the inshore boundary. The bottom picture shows stronger refraction than the middle picture which in turn shows stronger refraction than the top picture. This means that the ray separation increases substantially in the bottom picture (as can be seen directly from the picture) and therefore that the wave height will be considerably reduced. Proportionately smaller reductions in wave height occur in the other two pictures. Despite this refraction effect, it turns out that the bottom picture is the correct answer to our question - it actually gives larger wave heights than the middle picture, which in turn gives larger wave heights than the top picture.

The reason is due to the strong effects of shoaling and to a lesser extent the Doppler shift. In the bottom picture we have a large initial c_{ga} due to the c_{gr} and a large current acting together. This becomes significantly reduced at the inshore boundary as the current is reduced to a quarter of its starting value. We therefore get a large shoaling factor. In the top picture, however, the initial c_{gr} and current oppose each other giving a smaller initial c_{ga}. This decreases at the far boundary, but by a lesser amount than in the previous case. A smaller shoaling factor is therefore obtained. The Doppler factors show similar though smaller trends. The differences in the shoaling and Doppler factors are sufficiently strong to outweigh the differences in the refraction factors. Table 5 gives the refraction, shoaling and Doppler coefficients for the three cases.

This example shows that simple reasoning and desk calculations, which can often give a good qualitative idea of depth refraction, are unlikely to be reliable in the more complex task of predicting current-depth refraction. We would recommend the use of proper numerical modelling for such problems.

6 SUMMARY AND CONCLUSIONS

This report has considered the numerical modelling of the effects of currents on wave propagation. The theory of current-depth refraction of waves has been developed within the framework of time-independent and vertically uniform currents, and linear refraction theory for waves. Three types of pure-wave refraction model, namely the forward-

tracking and back-tracking ray models and the finite difference model, have been extended to include the effects of currents. Tests have been carried out on a simple depth grid which demonstrate that each of the models gives correct predictions of wave heights and directions. These tests showed that some surprising results can occur even in the simple examples considered, and they highlight the need for proper numerical modelling of wave-current problems.

These models are designed to be used in quite general coastal situations, though they should be used seawards of the breaker zone and where depth changes are gradual and regular. There are no restrictions on grid size, provided that the bathymetry and current field are adequately represented. Waves of any period and sea areas of any size can be modelled.

7 ACKNOWLEDGEMENTS

This study was carried out by Mr H N Southgate of Dr A H Brampton's Coastal Processes Section. This section is part of the Coastal Engineering Group headed by Mr M W Owen. This group is in the Maritime Engineering Department of Hydraulics Research Limited, headed by Dr S W Huntington.

8 REFERENCES

1. I G JONSSON, J B CHRISTOFFERSEN and O SKOVGAARD "A general computational method for current-depth refraction of water waves" International Conference on Coastal and Port Engineering in Developing Countries, Colombo, Sri Lanka, March 1983.

2. D H PEREGRINE and I G JONSSON "Interaction of waves and currents" Miscellaneous Report No 83-6, US Army, Corps of Engineers, Coastal Engineering Research Centre, March 1983.

3. I G JONSSON and J B CHRISTOFFERSEN "The complete equations for current-depth refraction of water waves" Progress Report 57, pp13-24, IHHE, Technical University of Denmark, November 1982.

4. H N SOUTHGATE "Ray methods for combined refraction and diffraction problems" Report IT 214, Hydraulics Research Limited, July 1981.

5. H N SOUTHGATE "A harbor ray model of wave refraction - diffraction" Journal of the Waterway, Port, Coastal and Ocean Engineering Division, ASCE, January 1985.

6. E C BOWERS and H N SOUTHGATE "Wave refraction, diffraction and reflection. A comparison between a physical model and a mathematical ray model" Report IT 240, Hydraulics Research Limited, November 1982.

7. A H BRAMPTON "A computer method for wave refraction" Report IT 172, Hydraulics Research Limited, December 1977.

8. C L ABERNETHY and G GILBERT "Refraction of wave spectra" Report IT 117, Hydraulics Research Limited, May 1975.

9. H N SOUTHGATE "A finite difference wave refraction model" Report EX 1163, Hydraulics Reserach Limited, April 1984.

10. I G JONSSON "Booij's current wave equation and the ray approximation" Progress Report 54, pp7-20, IHHE, Technical University of Denmark, August 1981.

11. D H PEREGRINE "Interaction of water waves and currents" Advances in Applied Mechanics, Vol 16, 1976.

12. H N SOUTHGATE "Techniques of ray averaging" International Journal for Numerical Methods in Fluids, Vol 4, August 1984.

13. I G JONSSON "The dynamics of waves on currents over a weakly varying bed" in Lecture Notes in Physics, Vol 64, Waves on Water of Variable Depth, Ed D G Provis and R Radok, 1977.

APPENDIX - LIST OF SYMBOLS

A	Wave height
b	Separation between neighbouring rays
c_{ga}	Absolute group velocity
c_{gr}	Relative group velocity
f	Co-ordinate direction along wave front
g	Acceleration due to gravity
h	Depth
k	Wavenumber
k_x	Component of wavenumber in x direction
k_y	Component of wavenumber in y direction
r	Co-ordinate direction along ray
s	Co-ordinate direction along wave orthogonal
S	Spectral density function
t	Time
T	Tanh (kh)
U	Current magnitude
U_x	Component of current in x direction
U_y	Component of current in y direction
x	Cartesian co-ordinate
y	Cartesian co-ordinate
α	Wave orthogonal direction
δ	Current direction
μ	Ray direction
ω_a	Absolute angular frequency
ω_r	Relative angular frequency
∇	Two dimensional gradient operator
$\underline{\ }$	(Underline) denotes vector quantities
$\cdot$	Scalar product of two vectors
$\times$	Vector product of two vectors (in Eq 1)

Ray, orthogonal and current directions measured anticlockwise from the x axis to the forward direction of the ray, orthogonal or current.

Tables

TABLE 1

INSHORE WAVE HEIGHT COEFFICIENTS. NO CURRENTS.

INCIDENT ORTHOGONAL DIRECTION (DEGREES RELATIVE TO X AXIS)	INSHORE WAVE HEIGHT COEFFICIENTS				
	BACK TRACKING RAY MODEL	FORWARD TRACKING RAY MODEL	FINITE DIFFERENCE MODEL		ANALYTICAL SOLUTION (SNELL'S LAW)
			One Corrector Step	Two Corrector Steps	
35	1.003	1.011	1.008	1.008	1.009
45	1.091	1.098	1.086	1.086	1.096
55	1.158	1.158	1.141	1.141	1.156
65	1.197	1.197	1.178	1.178	1.197
75	1.223	1.223	1.201	1.201	1.221
85	1.229	1.233	1.212	1.212	1.233
95	1.229	1.233	1.212	1.212	1.233
105	1.223	1.223	1.201	1.201	1.221
115	1.197	1.197	1.178	1.178	1.197
125	1.158	1.158	1.141	1.141	1.156
135	1.091	1.098	1.086	1.086	1.096
145	1.003	1.011	1.008	1.008	1.009

TABLE 2

INSHORE WAVE ORTHOGONAL DIRECTIONS. NO CURRENTS

INCIDENT ORTHOGONAL DIRECTION (DEGREES RELATIVE TO X AXIS)	INSHORE WAVE DIRECTIONS (DEGREES RELATIVE TO X AXIS)				
	BACK TRACKING RAY MODEL	FORWARD TRACKING RAY MODEL	FINITE DIFFERENCE MODEL		ANALYTICAL SOLUTION (SNELL'S LAW)
			One Corrector Step	Two Corrector Steps	
35	59.4	59.0	59.3	59.3	59.3
45	63.9	63.6	63.8	63.8	63.8
55	69.1	68.9	69.0	69.1	69.0
65	74.8	74.6	74.7	74.7	74.7
75	80.8	80.6	80.7	80.7	80.7
85	86.9	86.8	86.9	86.9	86.9
95	93.1	93.2	93.1	93.1	93.1
105	99.2	99.4	99.3	99.3	99.3
115	105.2	105.4	105.3	105.3	105.3
125	110.9	111.1	111.0	110.9	111.0
135	116.1	116.4	116.2	116.2	116.2
145	120.6	121.0	120.7	120.7	120.7

TABLE 3

INSHORE WAVE HEIGHT COEFFICIENTS. CURRENT TO LEFT

INCIDENT ORTHOGONAL DIRECTION (DEGREES RELATIVE TO X AXIS	INSHORE WAVE HEIGHT COEFFICIENTS						
	BACK TRACKING RAY MODEL		FORWARD TRACKING RAY MODEL		FINITE DIFFERENCE MODEL		ANALYTICAL SOLUTION (SNELL'S LAW WITH CURRENTS
	No Iteration	One Iteration	No Iteration	One Iteration	One Corrector Step	Two Corrector Steps	
35	0.930	0.929	0.942	0.939	0.936	0.936	0.948
45	1.005	1.004	1.022	1.019	1.012	1.012	1.026
55	1.073	1.082	1.086	1.084	1.073	1.073	1.089
65	1.129	1.138	1.140	1.139	1.124	1.124	1.142
75	1.177	1.176	1.186	1.185	1.166	1.166	1.185
85	1.214	1.225	1.222	1.222	1.200	1.200	1.219
95	1.232	1.245	1.247	1.247	1.223	1.223	1.242
105	1.256	1.257	1.258	1.258	1.233	1.233	1.250
115	1.257	1.257	1.252	1.252	1.227	1.227	1.241
125	1.224	1.227	1.223	1.224	1.202	1.202	1.211
135	1.175	1.176	1.167	1.167	1.153	1.153	1.154
145	1.083	1.083	1.077	1.077	1.077	1.077	1.063

TABLE 4

INSHORE WAVE ORTHOGONAL DIRECTIONS. CURRENT TO LEFT

INCIDENT ORTHOGONAL DIRECTION (DEGREES RELATIVE TO X AXIS)	INSHORE WAVE DIRECTIONS (DEGREES RELATIVE TO X AXIS)						
	BACK TRACKING RAY MODEL		FORWARD TRACKING RAY MODEL		FINITE DIFFERENCE MODEL		ANALYTICAL SOLUTION (SNELL'S LAW WITH CURRENTS)
	No Iteration	One Iteration	No Iteration	One Iteration	One Corrector Step	Two Corrector Steps	
35	52.1	51.8	51.4	51.7	51.7	51.7	51.8
45	59.0	58.6	58.4	58.7	58.7	58.7	58.8
55	66.1	65.9	65.6	65.9	65.9	65.9	66.0
65	73.1	73.0	72.9	73.0	73.0	73.0	73.2
75	80.0	80.0	79.9	80.0	80.0	79.9	80.2
85	86.5	86.6	86.7	86.6	86.6	86.6	86.8
95	92.6	92.8	93.0	92.8	92.8	92.8	93.1
105	98.3	98.6	98.6	98.6	98.6	98.6	98.8
115	103.5	103.8	104.3	103.8	103.8	103.8	104.1
125	108.1	108.5	109.0	108.5	108.5	108.5	108.8
135	112.2	112.5	113.1	112.6	112.6	112.6	112.8
145	115.4	115.9	116.5	116.0	115.9	116.0	116.1

TABLE 5

ANALYTICAL SOLUTION SHOWING REFRACTION, SHOALING AND DOPPLER COEFFICIENTS IN EACH CASE THE INCIDENT ORTHOGONAL DIRECTION IS 45°

TEST	INSHORE ORTHOGONAL DIRECTION (DEGREES RELATIVE TO X AXIS)	REFRACTION COEFFICIENT	SHOALING COEFFICIENT	DOPPLER COEFFICIENT	WAVE HEIGHT COEFFICIENT (PRODUCT OF COLUMNS 2, 3 AND 4)
Currents to left Fig 4 Top	58.7	0.984	1.119	0.932	1.026
No Currents Fig 4 Middle	63.8	0.888	1.235	1.000	1.097
Currents to right Fig 4 Bottom	67.2	0.811	1.340	1.062	1.154

Figures

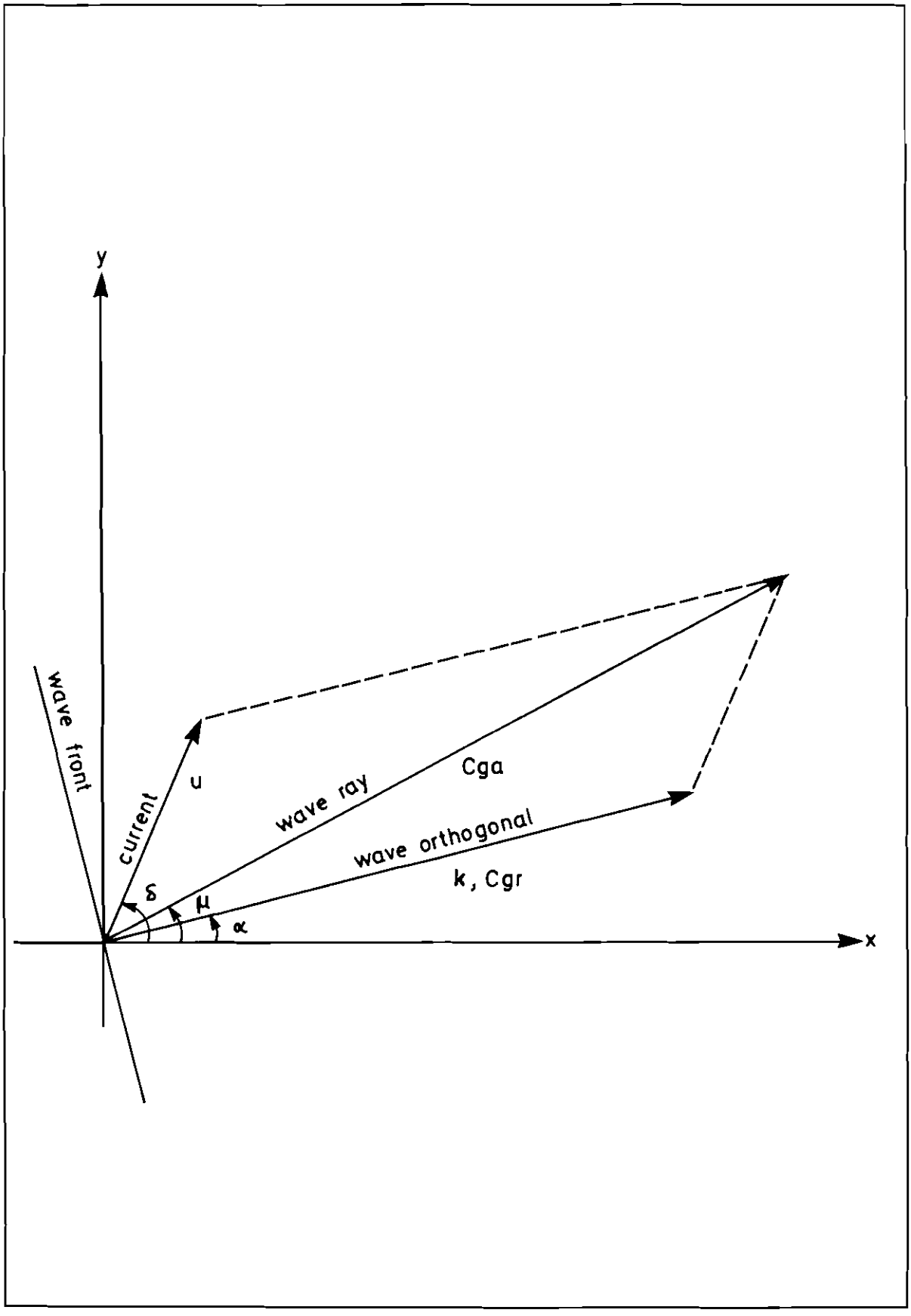

Fig 1 Geometry of currents, wave orthogonals and wave rays

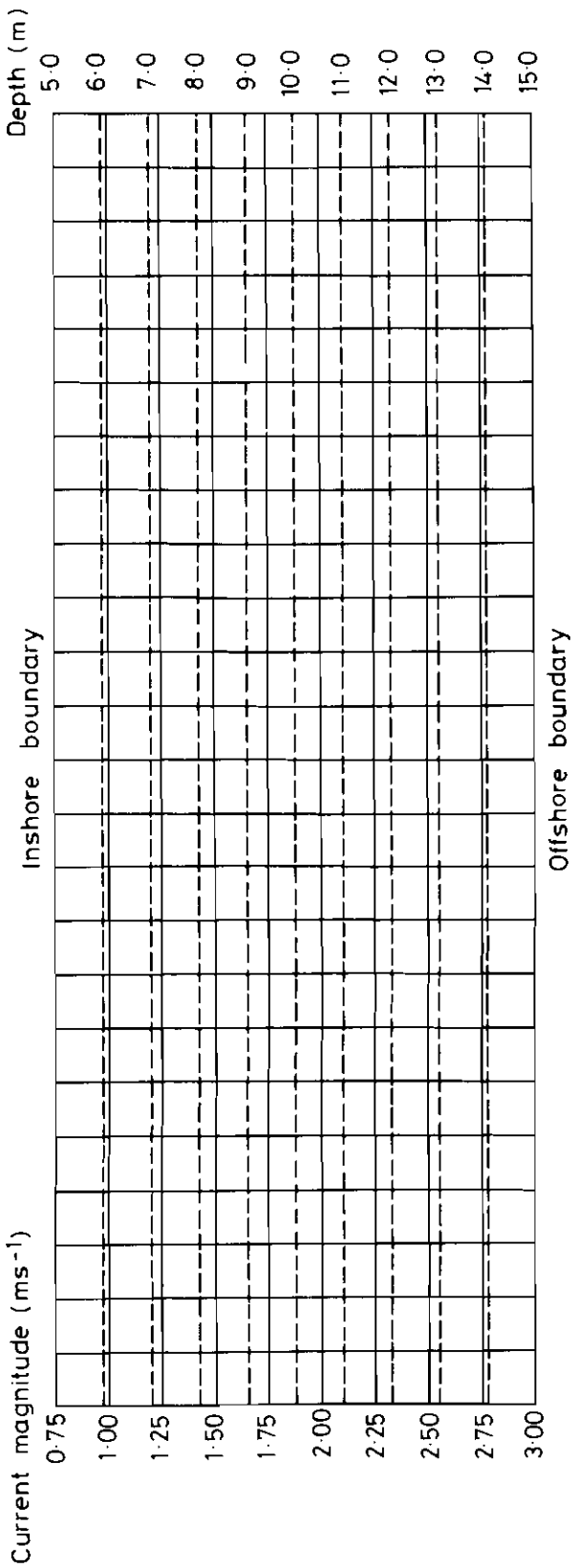

Fig 2 Computational model grid, depth contours and currents

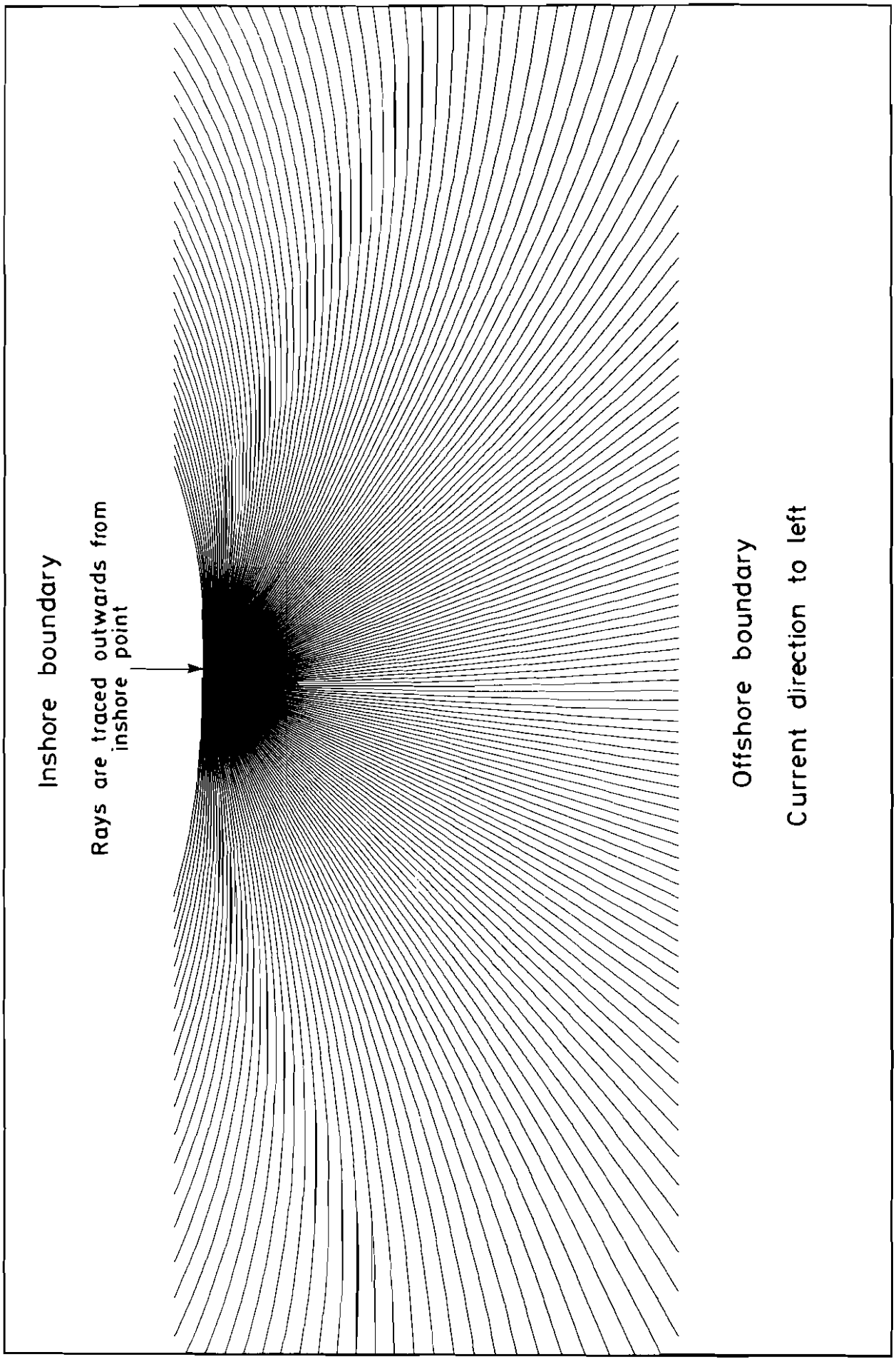

Fig 3 Back-tracking ray model. Ray paths.

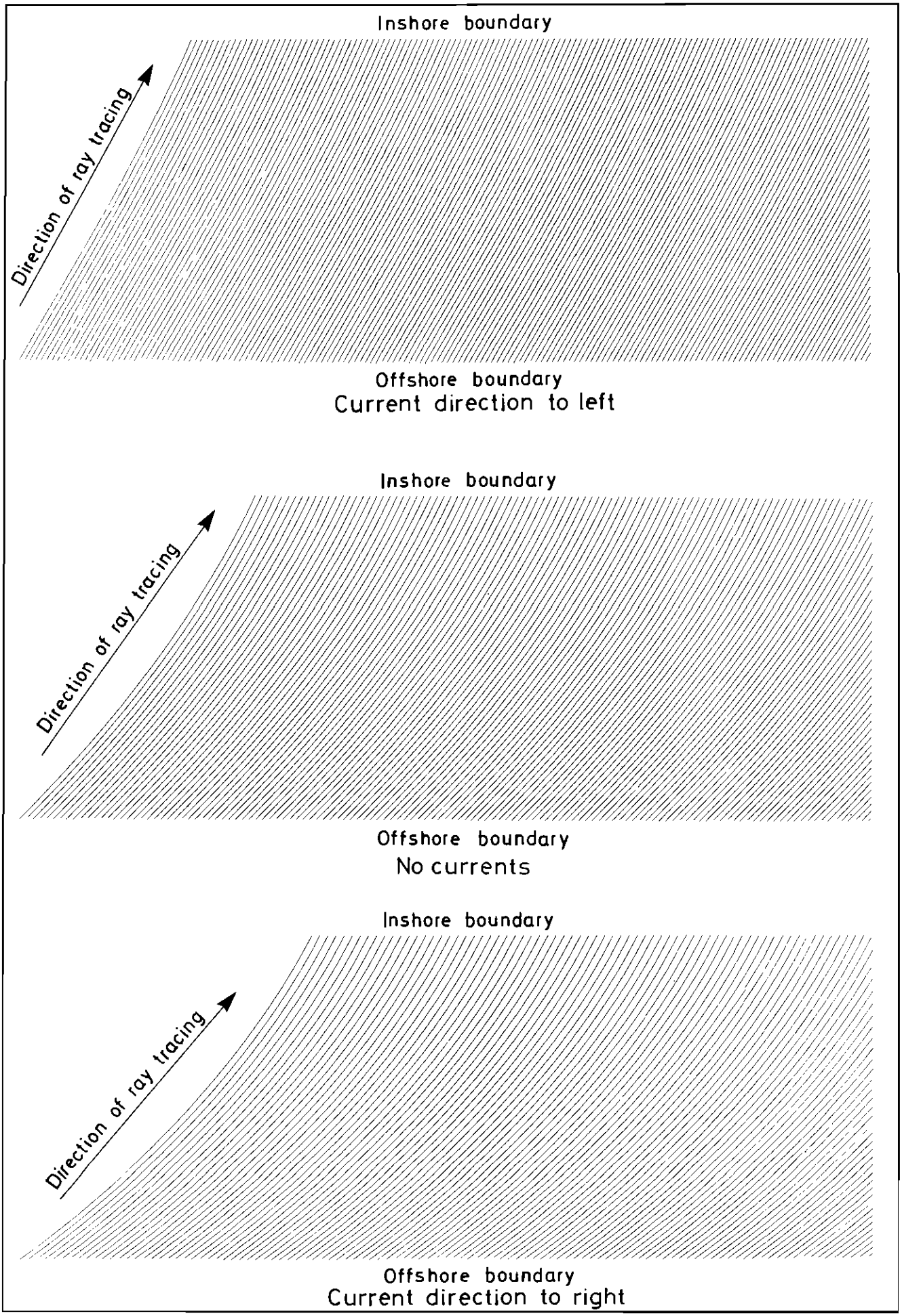

Fig 4 Forward-tracking ray model. Ray paths. Incident orthogonal direction 45°